Absolute polarization measurement of the 200 MeV proton beam at BNL Linac

A.A. Poblaguev[*][†]**, G. Atoian, and A. Zelenski**

Brookhaven National Laboratory, Upton, NY 11973, USA

E-mail: poblaguev@bnl.gov

For absolute calibration of the vertically polarized 200 MeV proton beam at BNL Linac, we detect in left/right symmetric scintillator detectors the elastic protons from the beam scattering on the Carbon target. The detectors are located at angles $\theta_{\text{Lab}} = \pm 16.2°$, at which analyzing power of the elastic scattering has local maximum of 99.35%. Variable length copper absorbers of ~ 40 mm thickness are installed in both arms of the polarimeter to suppress the inelastic protons. During RHIC Run 2017 we upgraded the polarimeter DAQ with a 250 MHz12 bit WFD. The detailed analysis of all detected events allowed us to properly isolate scattered proton signals and to control in-situ the efficiency of inelastic proton suppression. The systematic error in absolute polarization measurement was confirmed to be $\sigma_P^{\text{syst}}/P \sim 0.5\%$.

---

[*]Speaker.

1. Introduction

The polarized beam for RHIC spin physics experimental program at Brookhaven National Laboratory (BNL) is produced in the optically-pumped polarized H$^-$ ion source (OPPIS) [1] and then accelerated in a linear accelerator (Linac) to 200 MeV beam energy for strip-injection to the Booster and further accelerated to 24.3 GeV in AGS for injection in RHIC.

Precision, absolute polarization measurements in the wide energy range from a few keV (in the source) to 255 GeV (top RHIC energy) are required for accelerator tuning to minimize depolarization and finally for experimental data normalization. Therefore, the polarimetry is an essential component of the polarized collider facility. A complete set of polarimeters includes: Lamb-shift polarimeter at the source energy, a 200 MeV polarimeter [2] after the linac, and polarimeters in AGS and RHIC based on proton-Carbon scattering in Coulomb-Nuclear Interference region [3]. A polarized hydrogen jet polarimeter (HJET) was used for the absolute polarization measurements in RHIC [4].

The 200 MeV polarimeter initial design was based on proton-Carbon inclusive scattering at 12° angle. The polarimeter was calibrated to ±5% absolute accuracy in calibration experiment by comparison with proton-Deutron elastic scattering. The 12° polarimeter is used for the source development polarization tuning and optimization. The polarized source upgrade to 10 mA H$^-$ intensity and 85% polarization required more accurate absolute polarization measurements at very high peak intensities. The precision absolute measurements at injection to Booster and AGS are also essential for depolarization studies in Booster and AGS.
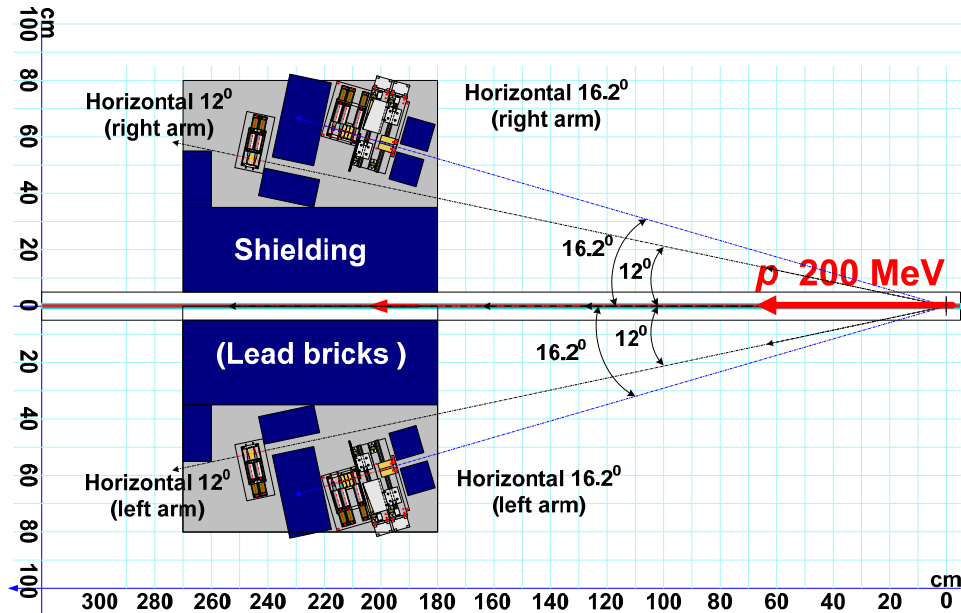

Figure 1: The 200 MeV polarimeter layout. The inclusive 12° polarimeter and elastic absolute 16.2° polarimeter are installed and aligned at the common table.

1

2. Analyzing power of 200 MeV proton-Carbon scattering

For scattering with spin structure $\frac{1}{2} + 0 \to \frac{1}{2} + 0$, it has been demonstrated [5] that the analyzing power can be *exactly* unity for certain combination of the beam energy T_0 and scattering angle θ_0. Such a case of $p + {}^{12}C$ scattering at $T_0 = 189 \pm 2$ MeV and $\theta_0^{lab} = 17.3° \pm 0.3°$ was precisely studied at IUCF [6]. Around the maximum, the analyzing power is adequately approximated [7] by

$$A_N(T, \theta) = 1 - \alpha (T - T_0)^2 - \beta (T - T_0)(\theta - \theta_0) - \gamma (\theta - \theta_0)^2 \qquad (2.1)$$

with coefficients

$$\begin{aligned}
\alpha &= (1.21 \pm 0.07) \times 10^{-4} \ \text{MeV}^{-2} \\
\beta &= (1.61 \pm 0.11) \times 10^{-3} \ \text{MeV}^{-1}\text{deg}^{-1} \\
\gamma &= (1.00 \pm 0.07) \times 10^{-2} \ \text{deg}^{-2}
\end{aligned} \qquad (2.2)$$

For 200 MeV beam, the analyzing power reaches a maximum

$$A_N(200 \text{ MeV}, 16.2°) = (99.35 \pm 0.15)\% \qquad (2.3)$$

at the scattering angle $\theta = 16.2°$. Employing this angle for absolute measurement of 200 MeV proton beam polarization has obvious advantages: *(i)* the analyzing power is close to 1 and is known with very high precision and *(ii)* the measurement is not sensitive to possible misalignment of the detectors position angles.

In this situation backgrounds, particularly inelastic ($\Delta > 0$) scattering

$$p + C \to p + C^*, \quad \Delta = M_{C^*} - M_C \qquad (2.4)$$

become the main limiting factor for such an absolute polarimeter. Comparison of analyzing powers and cross-sections for elastic and inelastic $p^\uparrow C$ scattering is shown in Fig. 2. For the 16.2° scattering angle, the $\Delta = 4.44$ MeV inelastic events dilute the analyzing power by $\sim 2\%$.
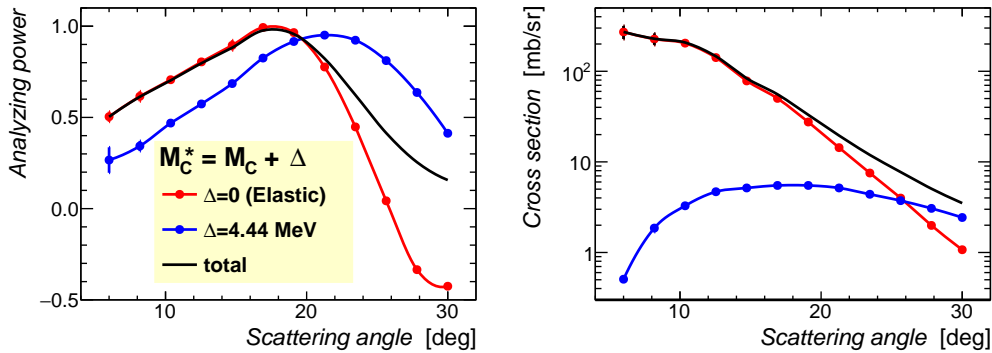

Figure 2: Analyzing power [6] (left) and cross-section [8] (right) for 200 MeV proton scattering on Carbon target. The red color is for elastic scattering and blue is for $\Delta = 4.4$ MeV inelastic one.
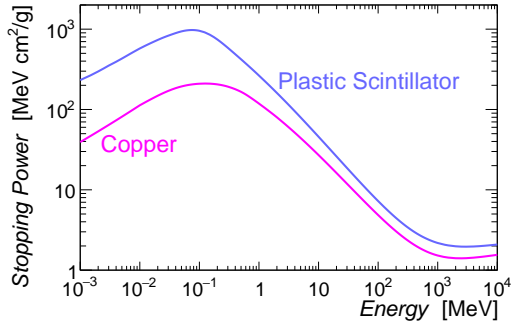
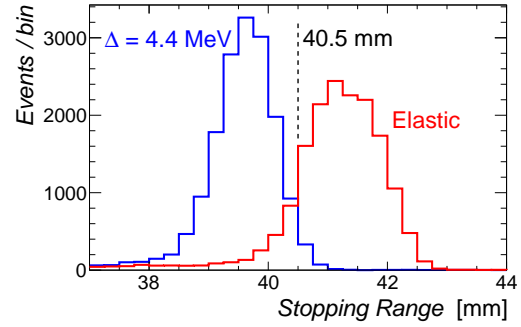**Figure 3:**　Proton stopping sower in copper and plastic scintillator [9]

Figure 4:　Geant simulation of the stopping range distributions for the elastic and inelastic protons in copper absorber [10]

3. The 16.2 degree polarimeter

The 200 MeV inclusive polarimeter was upgraded and calibrated in the 2009 Run to absolute accuracy better than $\pm 0.5\%$ by using the proton-Carbon elastic scattering measurements in additional $16.2°$ arms [11].

To suppress the inelastic background, a very simple and efficient method was developed. At $16.2°$ the scattered proton energy depends on Δ as

Δ [MeV]	0 (elastic)	4.44	7.65
T [MeV]	198.5	194.1	190.9

In spite of only a 2% gap between the elastic and inelastic energies, an absorber in the scattered proton path can efficiently isolate the elastic events due to a strong dependence of stopping power (see Fig. 3) on proton energy. The 194.1 MeV inelastic proton has 41 mm stopping range in copper. After passing such an absorber, the 198.5 MeV elastic proton will have 29 MeV kinetic energy which is equivalent to 8 mm stopping range in plastic scintillator.

For copper, Geant simulation of the stopping range distribution for elastic (198.5 MeV) and inelastic (194.1 MeV) protons is shown in Fig. 4. For a 40.5 mm Copper absorber, more than 80% of elastic protons will punch through the absorber while most of the inelastic protons will be stopped by it. The effective dilution of the elastic analyzing power only be 0.06% in this case.

The layout of the detector block (one arm) for the polarimeter tuned to $16.2°$ is shown in Fig. 5. (The scintillator #2 was installed at the end of Run 2017.)

Beam protons hit a thin Carbon target (about 4 mm in width and 100 μm in thickness). A collimated beam of scattered protons goes to consequently arranged plastic scintillation detectors. In order to adjust experimentally the absorber thickness, a stepwise absorber of variable thickness (0.5 mm step) was used in addition to the 38.1 mm fixed-length copper absorber.

The environmental (i.e. irrelevant to actual signal processing) systematic error of the spin asymmetry measurements was evaluated [10] as

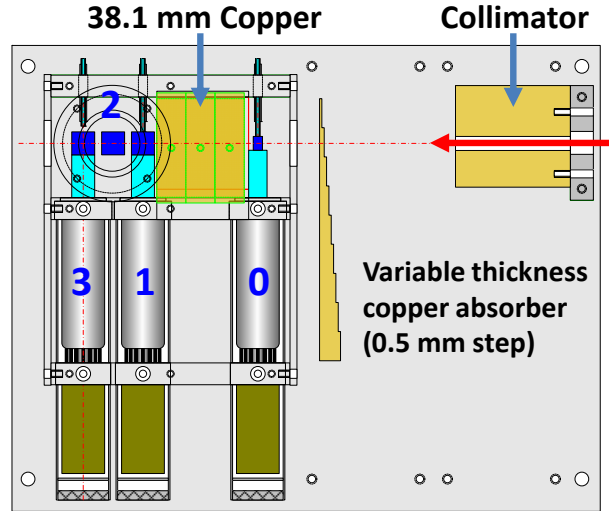$$(\sigma_P/P)_{\text{env}} = 0.2\% \tag{3.1}$$

Figure 5: Telescope of scintillation counters with an absorber for the 16.2° polarimeter.

This value includes contributions from the scintillator counters alignment, size of the scintillators, variations of beam energy, and multiple scattering in target, vacuum wall, and air.

Fast Hamamatsu photomultiplier tube with fast scintillator BC-404 gave the output pulse less than 15 ns. A coincidence signal is formed in vicinity of the detector in the beam line by fast discriminators.

The spin correlated asymmetry was calculated in a standard way by comparing rates in left/right arms depending on the beam spin direction. By variation of the absorber thickness, it was experimentally determined that the spin correlated asymmetry goes to plateau if the absorber is thicker than 40.5 mm. This evidently means full suppression of the inelastic protons. The systematic error of the absolute polarization measurement was evaluated to be

$$(\sigma_P/P)_{\text{syst}} = 0.5\% \tag{3.2}$$

including uncertainty in the analyzing power (2.3) and environmental (3.1) systematic error.

The 16.2° elastic polarimeter was employed for calibration of the 12° polarimeter used for online polarization tuning and monitoring.

4. The 16.2 degree polarimeter upgrade in RHIC Run 2017

In the 200 MeV polarimeter, the data readout is done by means of scalers. During many years of the polarimeter operation, this simple method was found to be sufficiently adequate for the polarimeter goals. However, since the beam intensity was significantly increased within the last few years, we decided to upgrade the 16.2° polarimeter with WFD readout to have permanent control for the rate and background effects. Also, the scintillator detectors behind the absorbers were
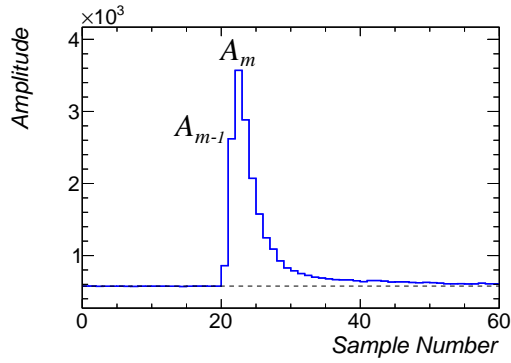
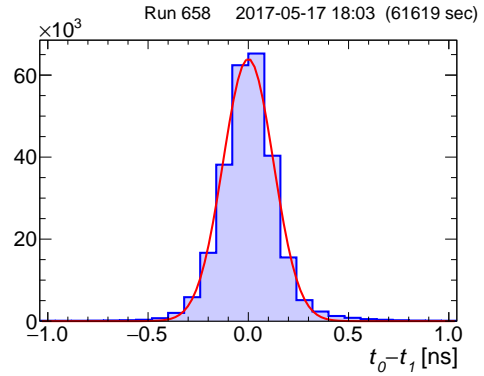**Figure 6:** A typical signal waveform. The time unit (sample number) is 4 ns.

Figure 7: The measured signal time difference in the scintillators #0 and #1.

replaced by three new counters, $10 \times 10 \times 9.5$ mm^3, in each arm. However, scintillator counters #0, with dimensions $6 \times 6 \times 4$ mm^3 remained unchanged.

The new DAQ was based on NIM logic triggers and 250 MHz 12 bit WFD readout of the scintillator signals. For the WFD readout we adopted HJET software [12]. For the beam structure of 300 μs bunch every 4 s, the trigger rate was about ~100 kHz in the bunch.

A typical signal waveform distribution is shown in Fig. 6. Signal time was defined by the maximum amplitude sample number, *m*, with a fine correction based on the A_{m-1}/A_m ratio. This simple and fast method allowed us to measure signal time with accuracy ~100 ps (see Fig. 7).

Detection of the scattered beam proton in the scintillator telescope is schematically shown in Fig. 8. A proton with kinetic energy less than 31 MeV will be stopped in the first scintillator. For the energy range 31-46 MeV, it will be stopped in the second one. It should be noted, that a proton signal amplitude in plastic scintillator is, generally, a nonlinear function of the deposited energy. Thus, one should not expect that the measured amplitude has is proportional to the deposited energy and that the amplitude correlation looks *exactly* like the distribution in Fig. 8.
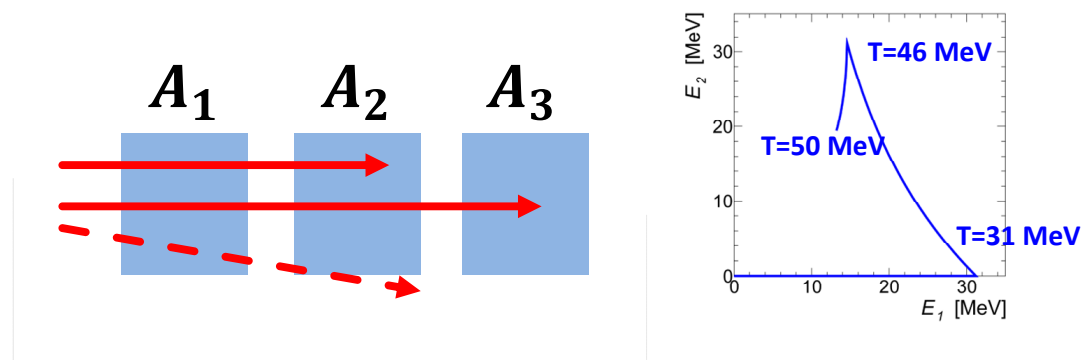

Figure 8: Left: A sketch of proton detection in a scintillator telescope. Right: Deposited energy correlation in the two consequent scintillator counters (9.5 mm of plastic scintillator each) depending of the proton entry energy.
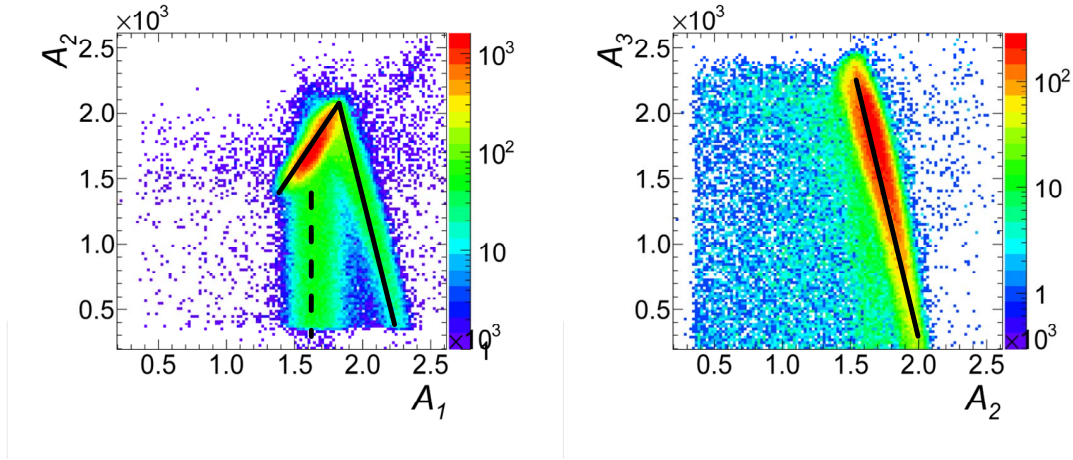
Figure 9: The measured signal amplitude correlation in scintillators 1-2 (left) and 2-3 (right). The results are for the minimal thickness absorber. The solid lines indicate scattered protons stopped in the scintillator telescope.

For the minimal thickness absorber (38.1 mm of copper and actually 4 mm of the scintillator), the measured signal amplitude correlations in scintillators 1-2 and 2-3 are shown in Fig. 9. We convincingly observe strong correlation between signal amplitudes which can be employed for background suppression. An excess of background events shown by the dotted line in the A_1-A_2 distribution can be associated with the side leakage in the telescope (Fig. 8).

In the study of the upgraded $16.2°$ polarimeter, a low threshold coincidence of signals in three scintillator 0,1,2 were used as a trigger. The trigger was independent for the left and right arms. One arm signal distributions for the minimal thickness absorber is shown in Fig. 10. The trigger thresholds can be easily identified on the plots. In this example, we selected events stopped in scintillator #3.

We studied spin asymmetry dependence on the total deposited energy in two consequent scintillators for two absorber thicknesses.

For the minimal thickness absorber, we studied the spin correlated asymmetry as a function of the sum $A_2 + A_3$ of amplitudes in scintillators #2 and #3. The results are shown in Fig. 11.
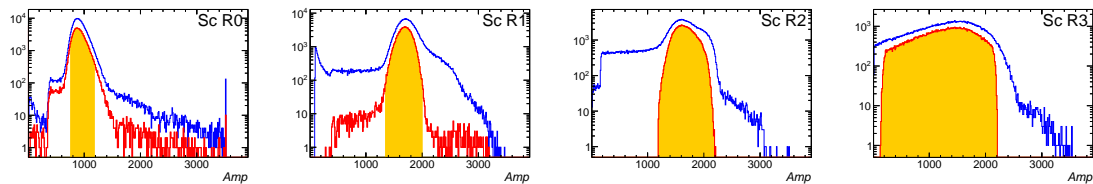

Figure 10: An example of the measured signal amplitude distributions for the minimal thickness absorber. Blue lines stand for distributions with no event selection cuts. Filled histograms show distributions with all cuts applied. The red lines mean that all cuts, except for the cut corresponding to the considered histogram, are applied.
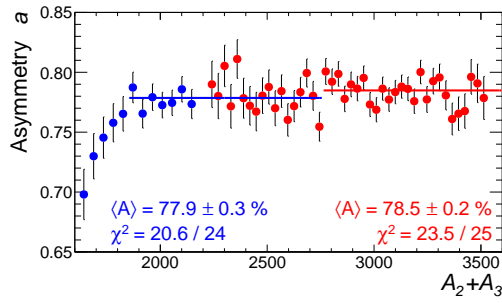
6

Figure 11: The measured spin asymmetry dependence on the amplitude sum $A_2 + A_3$. Blue markers indicate measurements with no signal in scintillator #3 ($A_3 = 0$). The variable absorber thickness was 0.0 mm.
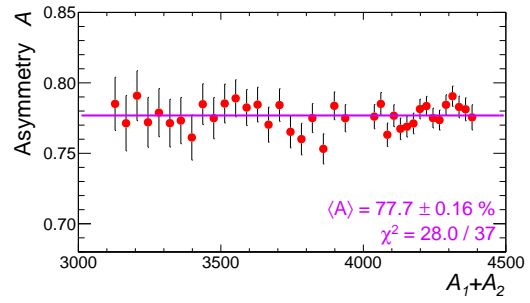

Figure 12: The measured spin asymmetry dependence on the amplitude sum $A_1 + A_2$. No detected signal in the scintillator #3. The variable absorber thickness was 1.5 mm.

A small difference (less than 2 standard deviations) between asymmetries in the $A_2 + A_3$ intervals 1800-2700 and 2800-3500 may be attributed to either the contribution of inelastic events or to a systematic error of about $\sim 0.4\%$ in the measurements.

For the 1.5 mm variable thickness absorber, the results are shown in Fig. 12. No evidence of the asymmetry dependence on the deposited energy was found which allows us to interpret these events as elastically scattered beam protons.

To evaluate systematic errors in measurements, we used events shown in Fig. 13. The projection to axis $\xi = A_1 + 0.45A_2$ is convenient for such a study because it minimize the width of the elastic signal distribution.

It was found that event rate distributions for spin up and down are essentially different (see Fig. 14) which, depending on the event selection cuts, may result in a strong systematic error in
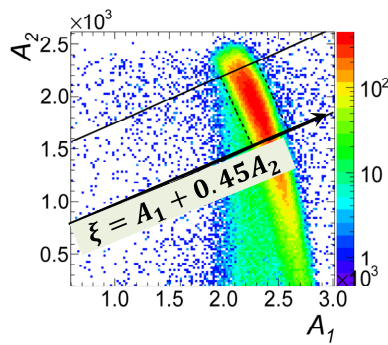

Figure 13: Event selection cuts (shown by solid black lines) to study systematic errors in the beam spin asymmetry measurements. The example is for measurements with the 1.5 mm variable thickness absorber.
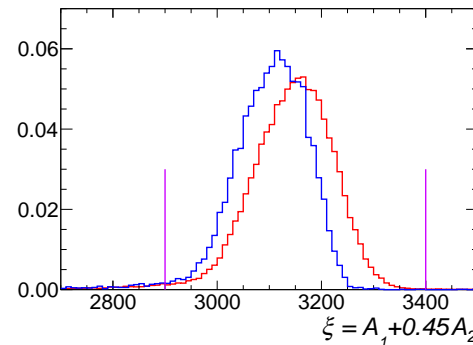

Figure 14: Normalized (unity integral) projection for the beam spin up (blue line) and down (red line). In this measurement, the spin down event rate in scintillators was about factor 10 higher than for spin up.
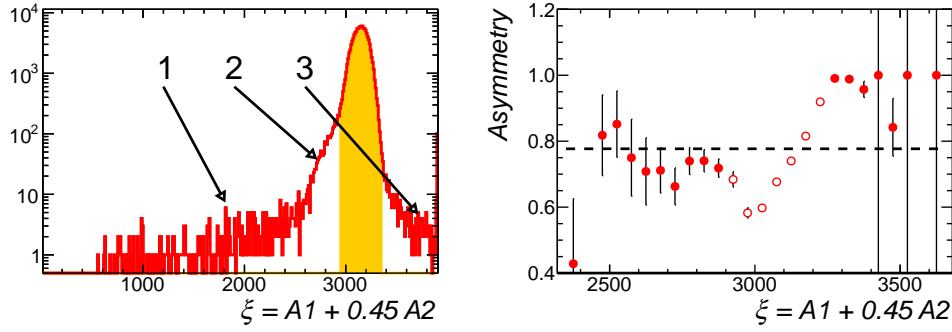
Figure 15: Left: Measured event rate projection to the ξ-axis. The evaluated backgrounds are enumerated. Right: Measured spin asymmetry as a function of ξ. Open circles correspond to the measurements strongly affected by the rate dependence.

polarization measurement. However, such an effect may be suppressed if both, spin up and down, distributions are within the (wide) event selection cut. For example, for the cuts shown in Fig. 14, the discussed systematic error is less than 0.1%.

Since the event rate in a polarimeter arm strongly depends on the beam polarization, we attribute the observed amplitude correlation with the beam spin to the signal amplitude dependence on the event rate in scintillator counter.

In the polarimeter upgrade study he have used two different scintillator types. The effect was observed only for one scintillator type. Also it was noticed that the observed amplitude-spin correlation was almost gone when the beam intensity was reduced by factor 4. More study of the issue is still needed.

For event selection cuts shown in Fig. 13, the measured event rate and spin asymmetry distributions are shown in Fig. 15. A background contribution to the effective analyzing power (and therefore to the systematic error of the beam polarization measurement) can be approximated as

$$\delta A_N^{\text{syst}} = \left(\left\langle A_N^{\text{bgr}} \right\rangle - A_N \right) \times f_{\text{bgr}} \tag{4.1}$$

where f_{bgr} is background the background fraction in the selected events.

For the backgrounds not correlated with the studied elastic events (1 and 3 in Fig. 15) one can evaluate $f_{\text{bgr}} \lesssim 0.001$. For the "side-leakage" background (2) $f_{\text{bgr}} \sim 0.05$. Considering the distribution of measured spin asymmetries, we can conclude

$$\sigma_{\text{syst}}^{\text{bgr}} \lesssim 0.3\% \tag{4.2}$$

Also, taking into account the uncertainty in the value of the analyzing power (2.3), environment related systematic errors (3.1) and actual statistical accuracy of the verification of the inelastic protons suppression, we can evaluate the systematic error of the absolute polarization measurement in the 16.2° degree polarimeter as

$$(\sigma_P/P)_{\text{syst}} \lesssim 0.6\% \tag{4.3}$$

5. Summary

The 16.2 degree absolute polarimeter at BNL Linac was upgraded to the WFD base DAQ. The first measurements with the upgraded polarimeter confirmed the previous result [11] that the Linac 200 MeV beam absolute polarization can be measured with systematic error of about $\sigma_P/P \sim 0.5\%$. The new DAQ allows us to adequately control the conditions of the measurements and, thus, makes the polarimeter easily adjustable to possible changes of the beam intensity, backgrounds, gains in photo-multipliers, etc.

Some improvements are still needed:

- Optimizing the scintillator counters, including the choice of scintillator material (in order to resolve the rate problem) and its dimensions.

- Optimization of the copper absorption thickness.

- Trigger less DAQ based on a 250 MHz WFD with a 300 μs (75k samples) readout capability.

We plan to continue studying/commissioning the 16 degree absolute polarimeter for the 200 MeV proton beam in RHIC Run 2019.

References

[1] A. Zelenski *et al.*, AIP Conf. Proc. **1869**, no. 1, 030015 (2017). doi:10.1063/1.4995735

[2] A. Zelenski *et al.*, J. Phys. Conf. Ser. **295**, 012132 (2011).

[3] H. Huang *et al.*, "AGS *p*-Carbon CNI Polarimeter Operation Experience.", in these proceedings.

[4] A.A. Poblaguev *et al.*, "HJET Polarimeter in RHIC Run 2017", in these proceedings.

[5] G. R. Plattner and A. D. Bacher, Phys. Lett. **36B**, 211 (1971).

[6] S. W. Wissink *et al.*, Phys. Rev. C **45**, R504 (1992).

[7] B. von Przewoski *et al.*, Phys. Rev. C **44**, 44 (1991).

[8] H. o. Meyer *at al.*, Phys. Rev. C **27**, 459 (1983).

[9] Shen, V.K., Siderius, D.W., Krekelberg, W.P., and Hatch, H.W., Eds., NIST Standard Reference Simulation Website, NIST Standard Reference Database Number 173, National Institute of Standards and Technology, Gaithersburg MD, 20899, http://doi.org/10.18434/T4M88Q

[10] G. Atoian *et al.*, PoS PSTP **2013**, 049 (2013).

[11] A. N. Zelenski *et al.*, Phys. Atom. Nucl. **76**, 1490 (2013) [Yad. Fiz. **76**, 574 (2013)].

[12] A. Poblaguev, PoS PSTP **2015**, 032 (2015).